

The quest for Type 2 quasars: Chandra observations of luminous obscured quasars in the Sloan Digital Sky Survey

Cristian Vignali,^{1,2*} Dave M. Alexander^{3*} and Andrea Comastri^{2*}

¹ Dipartimento di Astronomia, Università degli Studi di Bologna, Via Ranzani 1, 40127 Bologna, Italy

² INAF – Osservatorio Astronomico di Bologna, Via Ranzani 1, 40127 Bologna, Italy

³ Department of Physics, Durham University, South Road, Durham DH1 3LE

Accepted 2006 September 2. Received 2006 September 1; in original form 2006 July 6

ABSTRACT

We report on new *Chandra* exploratory observations of six candidate Type 2 quasars at $z=0.49\text{--}0.73$ selected among the most [O III] luminous emitters from the Sloan Digital Sky Survey (SDSS). Under the assumption that [O III] is a proxy for the intrinsic luminosity of the central source, their predicted rest-frame X-ray luminosities are $L_{2-10\text{keV}} \approx 10^{45} \text{ erg s}^{-1}$. For two of the targets, the photon statistics are good enough to allow for basic X-ray spectral analyses, which indicate the presence of intrinsic absorption ($\approx 10^{22-23} \text{ cm}^{-2}$) and luminous X-ray emission ($L_X \gtrsim 10^{44} \text{ erg s}^{-1}$). Of the remaining four targets, two are detected with only a few (3–6) X-ray counts, and two are undetected by *Chandra*. If these four sources have the large intrinsic X-ray luminosities predicted by the [O III] emission, then their nuclei must be heavily obscured ($N_H > \text{few} \times 10^{23} \text{ cm}^{-2}$) and some might be Compton thick ($N_H > 1.5 \times 10^{24} \text{ cm}^{-2}$). We also present the results for two Type 2 quasar candidates serendipitously lying in the fields of the *Chandra* targets, and provide an up-to-date compilation of the X-ray properties of eight additional SDSS Type 2 quasars from archival *Chandra* and XMM-Newton observations (five with moderate-quality X-ray data). The combined sample of 16 SDSS Type 2 quasars (10 X-ray detections) provides further evidence that a considerable fraction of optically selected Type 2 quasars are obscured in the X-ray band (at least all the objects with moderate-quality X-ray spectra), lending further support to the findings presented in Vignali, Alexander and Comastri (2004a) and unification schemes of Active Galactic Nuclei, and confirms the reliability of [O III] emission in predicting the X-ray emission in obscured quasars.

Key words: quasars: general — galaxies: nuclei — galaxies: active

1 INTRODUCTION

The quest for the identification of Type 2 quasars, the high-luminosity, long-sought after “big cousins” of local Seyfert 2 galaxies (i.e., characterized by high-ionization, narrow emission lines and a lack of broad emission lines in the rest-frame optical/ultraviolet spectra), has been the topic of numerous investigations over the past few years. Although there is not a unique definition of Type 2 quasars in the X-ray band, generally the most accepted view is that these sources should be the luminous and obscured ($L_X > 10^{44} \text{ erg s}^{-1}$ and $N_H > 10^{22} \text{ cm}^{-2}$) Active Galactic Nuclei (AGN) population predicted by unification schemes of AGN (e.g., Antonucci 1993) and required by many synthesis models of the X-ray background (XRB; e.g., Comastri et al. 2001; Gilli, Sal-

vati & Hasinger 2001). For example, in the most recent version of the synthesis model of Gilli, Comastri & Hasinger (2006), the contribution of Type 2 quasars to the XRB is estimated to be ≈ 15 per cent.

Over the past 4–5 years, deep X-ray surveys (such as those conducted in the *Chandra* deep fields; e.g., Giacconi et al. 2002; Alexander et al. 2003; see Brandt & Hasinger 2005 for a recent review) performed with *Chandra* and XMM-Newton have resolved a large fraction of the XRB (≈ 80 per cent in the 2–10 keV band; e.g., Bauer et al. 2004; Hickox & Markevitch 2006; but see also Worsley et al. 2005) and detected many high-redshift Type 2 quasar candidates (e.g., Crawford et al. 2001, 2002; Mainieri et al. 2002; Barger et al. 2003). Optical and infrared spectroscopy is critical to determine the redshifts of these sources and confirm that these candidates are “genuine” Type 2 quasars (i.e., matching both the optical and X-ray definitions). However, the majority of these objects are optically faint (most likely because they lie at high redshifts) and

* E-mail: cristian.vignali@oabo.inaf.it (CV); d.m.alexander@dur.ac.uk (DMA); andrea.comastri@oabo.inaf.it (AC).

are therefore challenging targets to obtain spectroscopic redshifts. As a consequence, although considerable efforts have been made, the number of spectroscopically confirmed Type 2 quasars from these surveys is comparatively small (e.g., Norman et al. 2002; Stern et al. 2002; Fiore et al. 2003; Perola et al. 2004; Gandhi et al. 2004; Caccianiga et al. 2004; Szokoly et al. 2004; Mainieri et al. 2005a; Maiolino et al. 2006), despite the fact that as many as 15–20 per cent of luminous obscured quasars are predicted to be observed in the deepest X-ray surveys (Alexander et al. 2001; Mainieri et al. 2005b).

The goal of our project is to select optically luminous Type 2 quasar candidates identified on the basis of high $[\text{O III}]\lambda 5007\text{\AA}$ luminosity from the ground-based, large-area Sloan Digital Sky Survey (SDSS; York et al. 2000) spectroscopic data and then follow up these sources with X-ray observations to confirm whether or not they are luminous and obscured also in the X-ray band. The advantage of this approach, compared to the study of Type 2 quasars found in moderately deep and ultra-deep X-ray surveys, is that at the optical magnitude limit of the SDSS, Type 2 quasars are generally easy to study at both optical and X-ray wavelengths. In addition, X-ray studies of optically selected Type 2 quasars can explore whether selection in the optical and X-ray bands identifies sources with intrinsically different properties. Due to observational limitations (e.g., small-size samples, low percentages of spectroscopic identifications, limited regions of the sky being surveyed), such studies have been challenging or impossible in the past.

In this paper we extend the work presented by Vignali, Alexander and Comastri (2004a, hereafter V04; 2004b) and focus on the study of the X-ray properties of Type 2 quasar candidates originally selected from the SDSS in the redshift range $\approx 0.3\text{--}0.8$. These sources are classified on the basis of high-excitation, narrow emission lines without underlying broad components and with line ratios characteristic of non-stellar ionizing radiation (Zakamska et al. 2003; see Zakamska et al. 2004, 2005 and 2006 for observations of these objects at other wavelengths). From the analysis of archival *ROSAT* and *XMM-Newton* observations, V04 were able to place constraints in a statistical sense on the X-ray emission of 17 of these objects (three X-ray detections and 14 upper limits). Assuming the correlation between the $[\text{O III}]$ and the 2–10 keV flux found for Seyfert 2 galaxies (Mulchaey et al. 1994) and adopting the parameterization reported in §3.2 of Collinge & Brandt (2000), V04 found that at least 47 per cent of the observed sample showed indications of X-ray absorption, including the four highest luminosity sources with predicted intrinsic luminosities of $\approx 10^{45}$ erg s^{-1} .

Here we present the exploratory *Chandra* observations for six additional SDSS Type 2 quasar candidates and provide an up-to-date list of the X-ray properties of Type 2 quasar candidates for which archival *Chandra* and *XMM-Newton* data are available (see also Ptak et al. 2006, hereafter P06, where pointed and archival X-ray observations of a sample of mostly bright SDSS Type 2 quasar candidates are presented). In total we have 16 sources (10 X-ray detections) with available *Chandra* and *XMM-Newton* data at present. The choice of *Chandra* and *XMM-Newton* is motivated by their broad-band coverage (thus minimizing the uncertainties due to extrapolations as in the case of *ROSAT* data), relatively large field-of-view, spectroscopic capabilities, and good sensitivity to relatively X-ray faint sources.

Hereafter we adopt the ‘‘concordance’’ (WMAP) cosmology ($H_0=70$ km s^{-1} Mpc $^{-1}$, $\Omega_M=0.3$, and $\Omega_\Lambda=0.7$; Spergel et al. 2003).

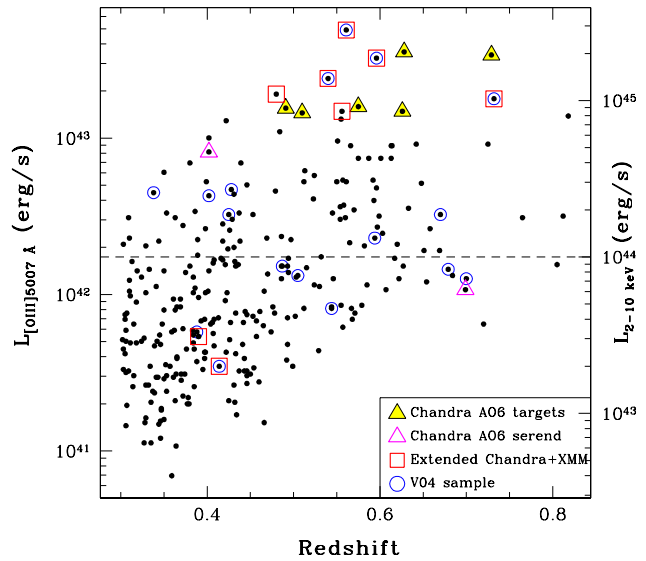


Figure 1. Logarithm of the measured $L_{[\text{O III}]}$ luminosities vs. redshift for all of the sources in the Zakamska et al. (2003) catalog (small filled circles). The y-axis on the right-hand side of the plot indicates the predicted 2–10 keV luminosity on the basis of the $[\text{O III}]$ emission (see §2.1). The dashed line provides an approximate separation between the locus of high-luminosity objects (quasar candidates, above the line) from that presumably populated by Seyfert galaxies (below the line); see Zakamska et al. (2003) for further details. The inset provides a key description of the X-ray observations.

2 THE MAIN SAMPLE: CHANDRA CYCLE 6 OBSERVATIONS

2.1 The sample selection

In the study conducted by V04, which used primarily *ROSAT* observations, ≈ 40 per cent of the Type 2 quasar candidates had predicted intrinsic 2–10 keV luminosities closer to those typically found for Seyfert galaxies than for quasars (open circles in Fig. 1; also see the summary of the results in Table 2 of V04). The principal goal of the work described here is to extend the study of V04 with the much higher sensitivity of *Chandra*. We selected six candidate Type 2 quasars on the basis of their luminous $[\text{O III}]$ emission which, in principle, should identify the most X-ray luminous members of the Type 2 quasar population (see filled triangles in Fig. 1). Even assuming the lowest X-ray luminosities predicted from the dispersion in the $L_{[\text{O III}]}$ – $L_{2-10 \text{ keV}}$ correlation, the six targets should still easily lie in the quasar regime ($L_{2-10 \text{ keV}} > 10^{44}$ erg s^{-1}). Hereafter we refer to this sample as the ‘‘main’’ *Chandra* sample.

2.2 Chandra data reduction and analysis

The six SDSS Type 2 quasar candidates were targeted by *Chandra* during Cycle 6 with the Advanced CCD Imaging Spectrometer (ACIS; Garmire et al. 2003) and the S3 CCD at the aimpoint, using short ($\approx 6.3\text{--}11.5$ ks) exposures. Standard data reduction procedures were adopted (see §2 of Vignali et al. 2005 for a detailed description) using the *Chandra* Interactive Analysis of Observations (CIAO) Version 3.2 software.

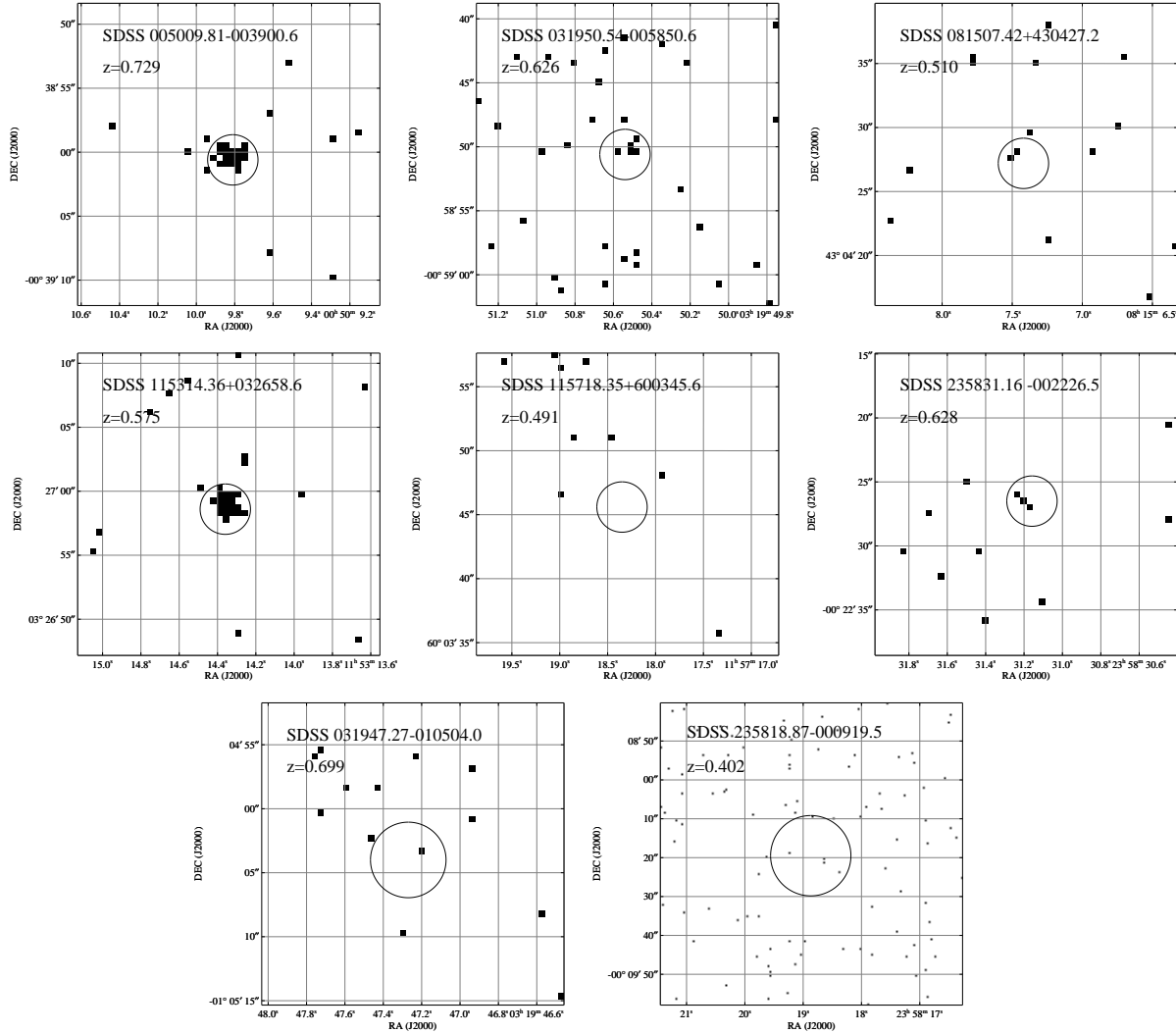


Figure 2. Full-band (0.5–8 keV) raw images of the quasars observed by *Chandra* in Cycle 6 and presented in this paper; the top six are the main targets and the bottom two are the serendipitous sources. The panels are $25'' \times 25''$ for all of the images, except for SDSS J2358–0009 ($\approx 80'' \times 80''$); North is up, and East to the left. For the six main targets, $2''$ -radius circles around the SDSS positions of the quasars are shown, while for the last two sources, which serendipitously fell within the *Chandra* field-of-view, the $3''$ -radius (SDSS J0319–0105) and $10''$ -radius (SDSS J2358–0009) source extraction regions are shown (see text for details). These two sources, along with two of the main targets, are not detected in the current *Chandra* observations.

Source detection was carried out with WAVDETECT (Freeman et al. 2002) using a false-positive probability threshold of 10^{-6} except for the faintest sources, where a false-positive probability threshold of 10^{-4} was adopted. The observation log is shown in Table 1; hereafter we will refer to the SDSS sources with their abbreviated names. For one source (SDSS J0319–0058), a high-background interval was removed from the *Chandra* observation, yielding a final useful exposure of 11.10 ks.

Four sources were detected with ≈ 3 –80 net counts in the observed 0.5–8 keV (full-band) energy range (see Table 2); their X-ray position is within $\approx 0.8''$ of the optical position (see Table 1), as expected given the positional accuracy of *Chandra* ACIS for on-axis observations. The 3-count source (SDSS J2358–0022) was detected using a false-positive probability threshold of 10^{-4} ; given the small number of pixels being searched due to the known source position and the sub-arcsec on-axis angular resolution of *Chandra*,

Table 1. SDSS Type 2 quasar candidates: *Chandra* and XMM-Newton observation logs.

Src. ID #	Object Name	z	X-ray (α_{2000})	X-ray (δ_{2000})	$\Delta_{\text{Opt-X}}$ (arcsec)	Obs. Date	Exp. Time (ks)	Off-axis (arcmin)	Seq. Num.
Sources observed as targets in <i>Chandra</i> AO6									
7	SDSS J005009.81-003900.6	0.729	00 50 09.8	-00 39 00.5	0.3	2005 Aug 28	7.85	0.0	701116
83	SDSS J031950.54-005850.6	0.626	03 19 50.5	-00 58 50.5	0.3	2005 Mar 10	11.10 ^a	0.0	701117
119	SDSS J081507.42+430427.2	0.510	2004 Dec 25	8.17	0.0	701118
196	SDSS J115314.36+032658.6	0.575	11 53 14.4	+03 26 58.6	0.3	2005 Apr 10-11	8.17	0.0	701119
197	SDSS J115718.35+600345.6	0.491	2005 Jun 03	6.97	0.0	701120
290	SDSS J235831.16-002226.5	0.628	23 58 31.2	-00 22 26.8	0.8	2005 Aug 08	6.27	0.0	701121
Serendipitous sources in <i>Chandra</i> AO6 observations									
82	SDSS J031947.27-010504.0	0.699	2005 Mar 10	9.67 ^{a,b}	7.4	701117
289	SDSS J235818.87-000919.5	0.402	2005 Aug 08	5.79 ^b	13.3	701121
Archival <i>Chandra</i> observations [targets+serendipitous sources]									
15	SDSS J011522.19+001518.5	0.390	01 15 22.2	+00 15 18.8	0.4	2002 Nov 01	33.70 ^b	2.1	800204
113	SDSS J080154.24+441234.0	0.556	08 01 54.3	+44 12 33.8	0.4	2003 Nov 27	9.82	0.0	701011
130	SDSS J084234.94+362503.1	0.561	1999 Oct 21	6.97 ^b	7.5	800040
207	SDSS J123215.81+020610.0	0.480	12 32 15.8	+02 06 10.4	0.4	2005 Apr 21	9.61	0.0	700992
Archival XMM-Newton observations [targets+serendipitous sources]									
34	SDSS J021047.01-100152.9	0.540	02 10 47.1	-10 01 54.1	1.7	2004 Jan 12-13	7.98/11.08/11.30 ^a	0.0	0204340201
59	SDSS J024309.79+000640.3	0.414	2000 Jul 29	14.89/19.44/16.93 ^{a,b}	10.4	0111200101
204	SDSS J122656.48+013124.3‡	0.732	12 26 56.5	+01 31 24.3	1.6	2001 Jun 23	6.17/5.49/7.37 ^{a,b}	6.0	0110990201
256	SDSS J164131.73+385840.9	0.596	16 41 31.7	+38 58 39.8	1.0	2004 Aug 20	12.20/16.51/16.61 ^a	0.0	0204340101

The source ID is taken from Table 1 of Zakamska et al. (2003). The optical positions of the quasars can be drawn from their SDSS name, while the X-ray positions for the X-ray detected sources have been obtained from WAVDETECT using the full-band image. All of the exposure times were corrected for detector dead time. For the XMM-Newton observations, all the exposure times of pn, MOS1, and MOS2 detectors are shown (after cleaning for the high-background periods). Results from archival *Chandra* and XMM-Newton observations were also reported in P06. ^a Corrected for high-background periods. ^b The exposure time has been obtained from the exposure map, since the source is not located on axis. ‡ Already presented by Vignali, Alexander and Comastri (2004).

the probability that this detection is spurious is low (2.8×10^{-4}). One target (SDSS J0815+4304) has 2 counts within a $2''$ -radius circle, but neither WAVDETECT nor Monte-Carlo simulations (giving a $\approx 3.5\sigma$ significance for this source being actually detected; see Vignali et al. 2005 for details on these simulations) provide conclusive support to the X-ray detection of this source.

Two additional SDSS Type 2 quasar candidates fell serendipitously in the field-of-view of the current *Chandra* observations (SDSS J0319-0105 and SDSS J2358-0009, plotted as open triangles in Fig. 1), at large off-axis angles ($7.4'$ and $13.3'$, respectively; see Table 1 for further details). None of them was detected with WAVDETECT up to false-positive probability thresholds of 10^{-3} . The photometric results for these two sources [adopting source extraction circles with radii of $3''$ and $10''$, respectively, to account for the broadening of the point spread function (PSF) at their large off-axis angles] are shown in Table 2.

The full-band raw (un-smoothed) images of the six main targets and two serendipitous sources are shown in Fig. 2.

2.3 X-ray spectral analysis: SDSS J0050-0039 and SDSS J1153+0326

Here we show the X-ray spectral results for the two targets with the most counts in the *Chandra* images analysed in this paper, SDSS J0050-0039 (≈ 41 full-band counts) and SDSS J1153+0326 (≈ 80 full-band counts; see Table 2). We look at the properties of the other sources in §3.

Spectral analysis was carried out with XSPEC Version 11.3.2 (Arnaud 1996) using unbinned data and the C -statistic (Cash 1979); given the low number of counts, this statistical approach is the most viable to provide basic constraints on the X-ray emission of these

Table 2. X-ray counts: *Chandra* observations

Source	Sample	X-ray counts			Count rate
		[0.5-2 keV]	[2-8 keV]	[0.5-8 keV]	[0.5-8 keV]
SDSS J0050-0039	M	$2.8^{+2.9}_{-1.6}$	$37.1^{+7.2}_{-6.1}$	$40.7^{+7.4}_{-6.4}$	$5.18^{+0.94}_{-0.81}$
SDSS J0319-0058	M	$2.0^{+2.7}_{-1.3}\ddagger$	$2.8^{+5.9}_{-1.6}$	$6.0^{+2.6}_{-2.4}$	$0.54^{+0.32}_{-0.22}$
SDSS J0815+4304	M	< 4.8	< 4.8	< 6.4*	< 0.78
SDSS J1153+0326	M	$38.4^{+7.3}_{-6.2}$	$42.2^{+7.6}_{-6.5}$	$80.4^{+10.1}_{-9.0}$	$9.84^{+1.26}_{-1.10}$
SDSS J1157+6003	M	< 3.0	< 3.0	< 3.0	< 0.43
SDSS J2358-0022	M	< 4.8	< 6.4‡	$2.9^{+2.9}_{-1.6}$	$0.46^{+0.46}_{-0.26}$
SDSS J0319-0105	S	< 3.0	< 4.4	< 4.4	< 0.50
SDSS J2358-0009	S	< 4.1	< 5.9	< 6.3	< 1.09
SDSS J0115+0015	A	$115.7^{+11.8}_{-10.7}$	$202.9^{+15.3}_{-14.2}$	$317.7^{+18.9}_{-17.8}$	$9.42^{+0.56}_{-0.53}$
SDSS J0801+4412	A	$4.9^{+3.4}_{-2.1}$	$33.3^{+6.8}_{-5.7}$	$38.1^{+7.2}_{-6.1}$	$3.88^{+0.73}_{-0.62}$
SDSS J0842+3625	A	< 9.9	< 6.6	< 7.7	< 1.11
SDSS J1232+0206	A	$2.0^{+2.7}_{-1.3}\ddagger$	$3.9^{+3.2}_{-1.9}$	$5.9^{+3.6}_{-2.4}$	$0.61^{+0.37}_{-0.25}$

“M” refers to the main target sample, “S” to the serendipitous sources and “A” to the archival sources. Errors on the X-ray net counts (i.e., background-subtracted) were computed according to Gehrels (1986). The upper limits are at the 95% confidence level and were computed according to Kraft, Burrows & Nousek (1991). Count rates are in units of 10^{-3} counts s^{-1} .

* The two X-ray counts in the source extraction region (see Fig. 2) are contiguous but neither WAVDETECT nor Monte-Carlo simulations provide conclusive support to the X-ray detection of this source, therefore an upper limit is reported according to Kraft et al. (1991). † The two X-ray counts are contiguous. ‡ The two X-ray counts are not contiguous, therefore an upper limit is reported according to Kraft et al. (1991).

sources (e.g., Nousek and Shue 1989) without losing spectral information (as, e.g., in the case of the hardness-ratio or band-ratio analyses). Errors are quoted at the 90 per cent confidence level for one interesting parameter ($\Delta C = 2.71$; Avni 1976; Cash 1979), un-

Table 3. Properties of the SDSS Type 2 quasars observed by *Chandra* and *XMM-Newton*.

Object (1)	$N_{\text{H,gal}}$ (2)	$\log L_{[\text{OIII}]}$ (3)	$F_{2-10 \text{ keV}}$ (4)	N_{H_z} (5)	$L_{2-10 \text{ keV}}$ (6)	$L_{2-10 \text{ keV}}$ (pr.) (7)	$S_{1.4 \text{ GHz}}$ (8)
SDSS J0050–0039	2.57	9.94	1.6×10^{-13}	$3.76^{+2.38}_{-1.58} \times 10^{23}$	7.2×10^{44}	$4.7 \times 10^{44} - 8.1 \times 10^{45}$	4.32
SDSS J0319–0058	6.05	9.58	2.2×10^{-15}	3.7×10^{42}	$2.0 \times 10^{44} - 3.6 \times 10^{45}$	< 0.143
SDSS J0815+4304*	5.03	9.57	< 3.1×10^{-15}	< 3.2×10^{42}	$2.0 \times 10^{44} - 3.5 \times 10^{45}$	6.09
SDSS J1153+0326	1.89	9.61	8.2×10^{-14}	$1.54^{+0.90}_{-0.54} \times 10^{22}$	1.2×10^{44}	$2.2 \times 10^{44} - 3.8 \times 10^{45}$	2.09
SDSS J1157+6003	1.65	9.60	< 1.6×10^{-15}	< 1.5×10^{42}	$2.1 \times 10^{44} - 3.7 \times 10^{45}$	1.54
SDSS J2358–0022	3.29	9.96	1.9×10^{-15}	3.2×10^{42}	$4.9 \times 10^{44} - 8.5 \times 10^{45}$	< 0.143
SDSS J0319–0105	5.92	8.44	< 2.9×10^{-15}	< 6.4×10^{42}	$1.5 \times 10^{43} - 2.6 \times 10^{44}$	< 0.137
SDSS J2358–0009	3.25	9.32	< 5.4×10^{-15}	< 3.1×10^{42}	$1.1 \times 10^{44} - 2.0 \times 10^{45}$	< 0.134
SDSS J0115+0015	3.42	8.14	1.3×10^{-13}	$3.25^{+0.64}_{-0.56} \times 10^{22}$	8.1×10^{43}	$7.4 \times 10^{42} - 1.3 \times 10^{44}$	< 0.150
SDSS J0801+4412	4.79	9.58	1.4×10^{-13}	$4.29^{+1.90}_{-2.10} \times 10^{23}$	4.2×10^{44}	$2.0 \times 10^{44} - 3.6 \times 10^{45}$	< 0.130
SDSS J0842+3625*	3.41	10.10	< 5.9×10^{-15}	< 7.7×10^{42}	$6.8 \times 10^{44} - 1.2 \times 10^{46}$	2.16
SDSS J1232+0206	1.80	9.69	2.3×10^{-15}	2.0×10^{42}	$2.6 \times 10^{44} - 4.6 \times 10^{45}$	< 1.117
SDSS J0210–1001	2.17	9.79	1.6×10^{-13}	$8.13^{+2.39}_{-1.92} \times 10^{22}$	2.2×10^{44}	$3.3 \times 10^{44} - 5.8 \times 10^{45}$	< 0.157
SDSS J0243+0006	3.56	7.95	< 3.6×10^{-15}	< 2.2×10^{42}	$4.8 \times 10^{42} - 8.3 \times 10^{43}$	< 0.276
SDSS J1226+0131	1.84	9.66	1.7×10^{-13}	$2.63^{+0.59}_{-0.47} \times 10^{22}$	4.3×10^{44}	$2.5 \times 10^{44} - 4.3 \times 10^{45}$	< 0.742
SDSS J1641+3858* †	1.16	9.92	4.5×10^{-13}	$5.51^{+0.47}_{-0.61} \times 10^{22}$	7.4×10^{44}	$4.5 \times 10^{44} - 7.8 \times 10^{45}$	3.54

(1) Abbreviated SDSS name; (2) Galactic column density, from Dickey & Lockman (1990), in units of 10^{20} cm^{-2} ; (3) \log of the [OIII] line luminosity, in units of L_{\odot} (from Zakamska et al. 2003); (4) Galactic absorption-corrected flux (or upper limit) in the 2–10 keV band, either extrapolated from the observed 0.5–8 keV (0.5–10 keV) count rate or upper limit in *Chandra* (*XMM-Newton*) observations, assuming a power law with $\Gamma = 2.0$ (typical for the AGN X-ray emission) or obtained directly from the X-ray spectral fitting (when possible) with Γ frozen to 2.0, for consistency with the other sources. The flux is in units of $\text{erg cm}^{-2} \text{ s}^{-1}$; (5) intrinsic column density, obtained from the X-ray spectral fitting and using a power law with $\Gamma = 2.0$, in units of cm^{-2} ; (6) 2–10 keV rest-frame luminosity, obtained through the observed flux (or upper limit), corrected for the effect of absorption (when the column density can be measured directly from the spectral fit), in units of erg s^{-1} ; (7) 2–10 keV luminosity range predicted from the [O III] line vs. hard X-ray flux correlation (Mulchaey et al. 1994; see also §2.1), in units of erg s^{-1} ; (8) radio flux density (or 1σ upper limits) at 1.4 GHz from the FIRST (Becker, White & Helfand 1995), in units of mJy. For SDSS J0050–0039 and SDSS J0815+4304, the radio flux densities reported here are the integrated values, while for the remaining radio-detected sources, the peak values are shown (since there is no evidence for extension in the radio band). We note that constraints on further 12 Type 2 quasar candidates (2 of which X-ray detected) are presented by V04.

* SDSS J0815+4304, SDSS J0842+3625 and SDSS J1641+3858 have “mean polarization” values (averaged over the observed 2820–6530Å band and uncorrected for the low dilution by the host galaxy) of 5.0, 15.4, and 4.6 per cent, respectively (Zakamska et al. 2005). In particular, spectro-polarimetry shows the presence of a broad H γ emission line in SDSS J0842+3625 and SDSS J1641+3858 ($FWHM \approx 4900$ and 3200 km s^{-1} , respectively) and narrow Mg II and H β emission lines (plus [O III]) in SDSS J0842+3625 (see Table 1 in Zakamska et al. 2005).

† For this source, the spectral parameters were obtained using a scattering model (with ≈ 3 per cent of scattered component), similarly to P06; the X-ray luminosity was corrected to account only for the nuclear emission.

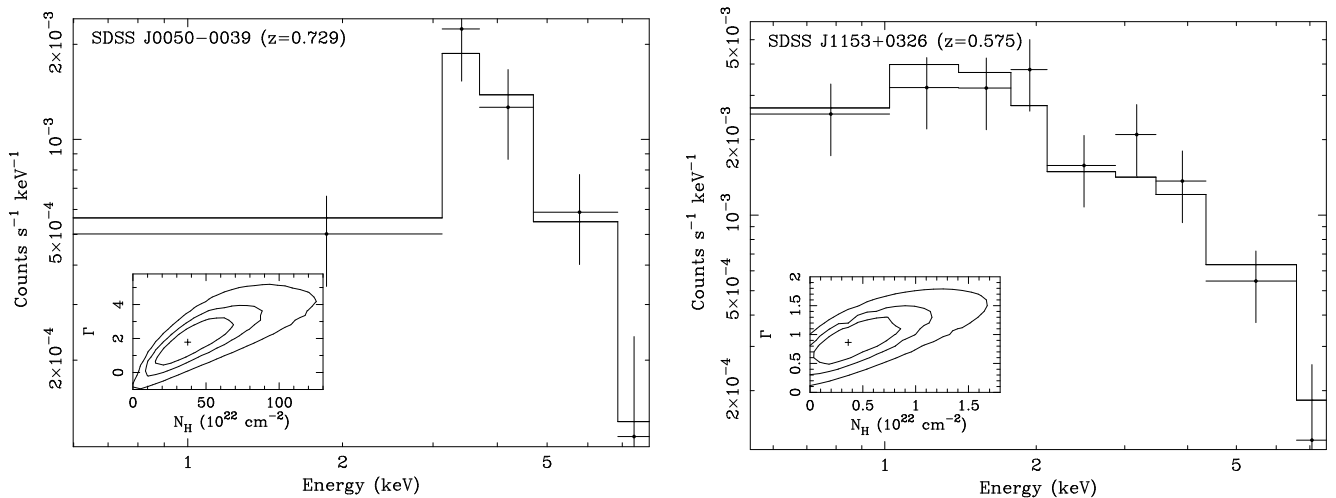


Figure 3. X-ray spectra of SDSS J0050–0039 (left panel) and SDSS J1153+0326 (right panel) fitted with an absorbed power-law model and the C -statistic; the data were rebinned for presentation purposes. The 68, 90, and 99 per cent confidence contours for the column density and photon index are shown in the insets (see §2.3 for details).

Table 4. X-ray counts: archival XMM-Newton observations.

	X-ray counts			Count rate
	pn	MOS1	MOS2	pn
SDSS J0210–1001	154	59	62	1.93±0.16
SDSS J0243+0006	< 29	< 22	< 18	< 0.20
SDSS J1226+0131	267	98	120	3.43±0.22
SDSS J1641+3858	963	411	412	7.89±0.27

Counts and count rates are computed in the 0.5–10 keV band; count rates are in units of 10^{-2} counts s^{-1} .

less stated otherwise. Initially, the two X-ray spectra are fitted with a power law and Galactic absorption only (from Dickey and Lockman 1990; see Table 3). In both cases, the flat photon index of the power-law component ($\Gamma = -0.78^{+0.50}_{-0.55}$ for SDSS J0050–0039 and $\Gamma = 0.56 \pm 0.28$ for SDSS J1153+0326) is suggestive of absorption, which is therefore included in the spectral fitting. Intrinsic absorption is statistically significant for SDSS J0050–0039 if Γ is left free to vary [$N_{\text{H}}(z = 0.729) = 3.75^{+3.12}_{-2.41} \times 10^{23} \text{ cm}^{-2}$, with $\Gamma = 1.78^{+1.22}_{-1.41}$; see Fig. 3],¹ while for SDSS J1153+0326 the implied absorption is $N_{\text{H}}(z = 0.575) = 1.54^{+0.90}_{-0.54} \times 10^{22} \text{ cm}^{-2}$ for a fixed photon index of $\Gamma = 2.0$ (as observed in local and high-redshift AGN; e.g., Reeves & Turner 2000; Piconcelli et al. 2005; Page et al. 2005; Shemmer et al. 2005, 2006). Given the presence of obscuration and the high de-absorbed, rest-frame 2–10 keV luminosities ($7.2 \times 10^{44} \text{ erg s}^{-1}$ and $1.2 \times 10^{44} \text{ erg s}^{-1}$ for SDSS J0050–0039 and SDSS J1153+0326, respectively) of these two sources, we conclude that both the X-ray and optical spectra indicate that these objects are Type 2 quasars.

3 THE “EXTENDED” SAMPLE: THE PROPERTIES OF SDSS TYPE 2 QUASARS

For our analyses of the overall properties of the SDSS Type 2 quasars, we extend the main (§2.1) and serendipitous (§2.2) samples with eight archival *Chandra* and XMM-Newton observations (open squares in Fig. 1); we remind that for the sources observed by *ROSAT* (see §1), a detailed analysis is presented in V04 and Vignali et al. (2004b), while the X-ray spectra of the sources with enough counts for X-ray fitting have been shown already in V04 and P06. Although the sources shown in this section (and summarized in Table 1) have already been published (V04; P06), we preferred to retrieve all the available X-ray data from the archives and perform a uniform analysis by adopting the same reduction techniques described in this paper (for the *Chandra* data) and in V04 (for the XMM-Newton data). We note that the agreement between our results and those of P06 is generally good.

We extracted the X-ray counts in the observed 0.5–8 keV energy range for *Chandra* (see Table 2) and in the observed 0.5–10 keV band for XMM-Newton (Table 4). For off-axis sources, we took into account the broadening of the PSF at the off-axis angles corresponding to the source position and, in the computation of the count rates reported in Tables 2 and 4, we adopted the exposure times derived from the exposure maps. At large off-axis angles (reported in Table 1), the difference with respect to the “nominal” exposure times can be significant (up to ≈ 50 per cent).

¹ The column density reported here is slightly different from that shown in Table 3, since the latter is obtained with $\Gamma = 2.0$.

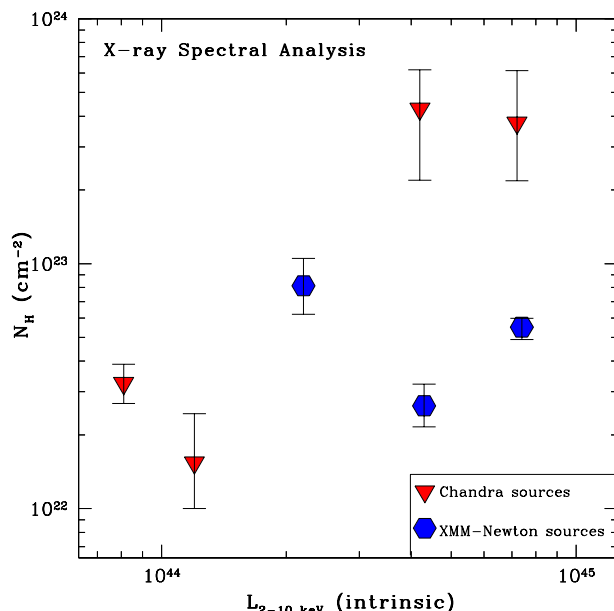


Figure 4. Intrinsic (de-absorbed) 2–10 keV luminosity vs. column density for the seven sources in the “extended” sample with enough counts for X-ray spectral analysis. The error bars represent the 90 per cent confidence level for the column density measurement.

3.1 Obscured and Compton-thick quasars

To draw some first results for the Type 2 quasars in the “extended” sample of 16 sources (Table 3), we compared their rest-frame, de-absorbed 2–10 keV luminosity (when a direct measurement of the column density from the X-ray spectrum is possible, see Fig. 5a; in the other cases, it is the measured X-ray luminosity, see Fig. 5b) with the X-ray luminosity range predicted by the Mulchaey et al. (1994) correlation (see §2.1).

All of the sources with enough counts for a basic or moderate-quality X-ray spectral analysis (seven in the current sample) are obscured, with column densities in the range $\approx 10^{22}$ – a few 10^{23} cm^{-2} (see Table 3 and Fig. 4). For two of these sources (the ones whose error bars do not touch the 1:1 dotted line in Fig. 5a), the de-absorbed 2–10 keV luminosities are below the lower bound of the predicted X-ray luminosity range. This might suggest that either absorption was not computed properly due to the limited photon statistics or the predictions from the [O III] line vs. hard X-ray flux correlation sometimes over-estimates the nuclear flux (see Netzer et al. 2006 for a discussion). We also point out that because of the limited wavelength coverage of the SDSS spectroscopy (≈ 2450 – 5900 \AA in the source rest frame at the average redshift of 0.56) it was not possible to estimate the reddening via the $H\alpha/H\beta$ Balmer decrement and therefore no corrections were applied to the [O III] flux to account for the absorption due to the narrow-line region itself (for details, see Maiolino et al. 1998; Bassani et al. 1999 and the recent results presented by Panessa et al. 2006); it is therefore possible that the prediction of the X-ray luminosity would be higher for at least some sources. A more detailed analysis on all these issues will be carried out when a larger sample of SDSS Type 2 quasars with good-quality X-ray spectra are available.

The situation appears different for the X-ray undetected sources and for those with a limited number of counts (Fig. 5b).

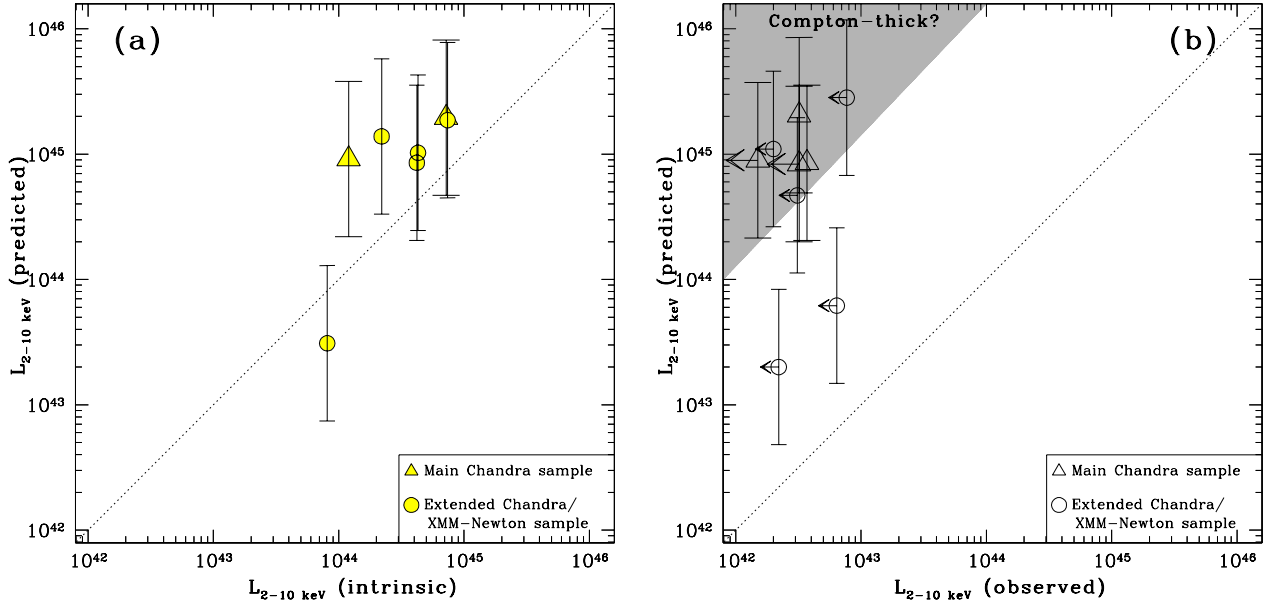


Figure 5. Comparison of the 2–10 keV luminosity computed from the available X-ray data with that predicted assuming the Mulchaey et al. (1994) correlation. The dotted line shows the 1:1 ratio between the two X-ray luminosities. (a) Sources whose X-ray luminosity is de-absorbed on the basis of the column density (N_{H} up to $\approx 5 \times 10^{23} \text{ cm}^{-2}$), computed directly from the X-ray spectra (see Table 3). (b) All of the remaining sources, for which the X-ray luminosity is derived from the X-ray flux with no correction for the unknown column density. Leftward arrows indicate upper limits on the observed X-ray luminosity, while the grey region shows the locus of extremely obscured, likely Compton-thick ($\gtrsim 10^{24} \text{ cm}^{-2}$) objects, where the observed luminosity is less than 1 per cent of the predicted one.

All of these sources have observed (i.e., not corrected for absorption) 2–10 keV luminosities generally far below (up to more than two orders of magnitude) the predicted X-ray luminosity range (see Table 3). On the basis of their optical spectra, there is no evidence that these sources host active nuclei of low luminosity and therefore the X-ray observations suggest that these sources are even more obscured than those for which X-ray absorption has been derived from direct X-ray spectral fitting. It is possible that the X-ray brightest sources are the “tip of the iceberg” of the SDSS Type 2 quasars, with $N_{\text{H}} \approx 10^{22}$ – a few 10^{23} cm^{-2} (Fig. 5a) and a significant fraction (up to ≈ 50 per cent) of the population is characterized by column densities $\gg 10^{23} \text{ cm}^{-2}$, with many Compton-thick ($N_{\text{H}} \gtrsim 10^{24} \text{ cm}^{-2}$) AGN (Fig. 5b; see P06 for similar conclusions). As further support to this indication, in Fig. 6 we plot the X-ray-to-[O III] flux ratio vs. column density for the 16 SDSS Type 2 quasars and the Seyfert 2 galaxies from the Bassani et al. (1999) and Guainazzi et al. (2005) compilations. While the SDSS Type 2 quasar candidates with direct column density measurements (filled triangles and circles) are in the obscured AGN region, most of the sources with lower photon statistics or undetected in the X-ray band (marked by dark and light-grey vertical lines, respectively, the latter with leftward-pointing arrows) lie in the $F_{\text{X}}/F_{[\text{OIII}]}$ region which is mostly populated by Compton-thick AGN. Provided that these results will be confirmed by further observations, there is evidence that the optical selection criteria adopted by Zakamska et al. (2003) on the basis of the SDSS spectra are highly effective in picking up moderate-redshift Compton-thick AGN.

3.2 Comparison with ROSAT results

Five sources are in common between the sample observed by *ROSAT* (V04) and the current “extended” sample (plotted as

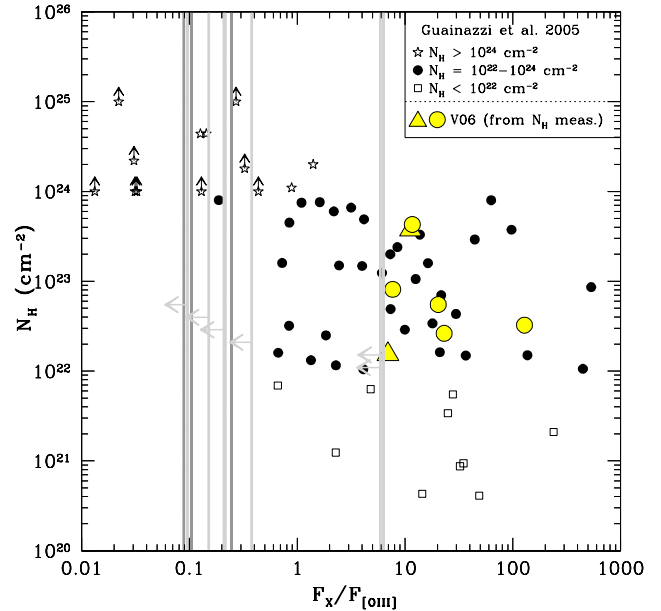


Figure 6. 2–10 keV-to-[O III] flux ratio vs. intrinsic column density for the sources presented in this paper (large filled triangles and circles, as in Fig. 5a) and the Seyfert 2 galaxies from Bassani et al. (1999) and Guainazzi et al. (2005). The X-ray fluxes are not corrected for absorption. Dark (light) grey regions indicate the X-ray-to-[O III] flux ratios for the sources with X-ray detections (upper limits, with leftward-pointing arrows) with no direct column density measurements.

Table 5. X-ray detections and upper limits vs. on-axis/off-axis observations.

On-axis observations				Off-axis observations			
<i>Chandra</i>		<i>XMM-Newton</i>		<i>Chandra</i>		<i>XMM-Newton</i>	
det	ul	det	ul	det	ul	det	ul
6(3)	2	2(2)	0	1(1)	3	1(1)	1

“det” means X-ray detection, while “ul” indicates an X-ray upper limit. The number of sources with available X-ray spectra (seven in the whole sample) is reported between parenthesis.

squared circles in Fig. 1): besides SDSS J1226+0131, whose *XMM-Newton* observation and spectrum were originally presented by V04, we find SDSS J0842+3625 (*Chandra* upper limit), SDSS J0210–1001 and SDSS J1641+3858 (both *XMM-Newton* detections with X-ray spectra available), and SDSS J0243+0006 (being undetected by *XMM-Newton* at a large off-axis angle). We note that the soft (0.5–2 keV) flux measurements obtained by the observations presented in this paper are deeper than those, relatively shallow, obtained by *ROSAT*, and are generally in agreement, with the exception of SDSS J1641+3858: for this source, the soft X-ray flux measured by *XMM-Newton* is a factor of ≈ 2 higher than the 3σ upper limit reported in V04. We note that it is possible that variability either in the nuclear/scattered flux or in the absorber might have occurred in the time interval between the *ROSAT* and *XMM-Newton* observations (≈ 11 years in the observed frame).

For all of these sources, the *ROSAT* analysis suggested the presence of absorption in the X-ray band (see Table 2 in V04), and the column densities obtained from X-ray spectral fitting (Table 3) are generally consistent, within the uncertainties, with those derived using *ROSAT* data.

3.3 Estimate of the number density of SDSS Type 2 quasars

Overall, it appears clear that the SDSS is able to provide a large sample of optically selected Type 2 quasars which are confirmed as such by X-ray observations and, possibly, a significant number of candidate Compton-thick AGN. To estimate the role of these Type 2 quasars in the AGN synthesis models for the XRB, it is compelling to derive their surface density and luminosity function and to extend the X-ray spectral analysis carried out in this paper to a larger sample. At present, given the highly inhomogeneous selection and incompleteness of the sample of 291 Type 2 AGN candidates presented by Zakamska et al. (2003), the number density of these objects is subject to large uncertainties and has not been accurately calculated yet. However, we can provide a first-order estimation. If we consider that 48.5 per cent of the plates used by Zakamska et al. (2003) were taken from the SDSS Data Release 1 (Abazajian et al. 2003), whose spectroscopic coverage is 1360 deg^2 , and assume that the SDSS Type 2 AGN are uniformly distributed, then their surface density would be $\approx 0.1 \text{ deg}^{-2}$. Since only approximately half of the sample can be associated with high-luminosity AGN on the basis of the [O III] luminosity (see §6.2 of Zakamska et al. 2003), the resulting estimate of the surface density of SDSS Type 2 quasars is $\approx 0.05 \text{ deg}^{-2}$. At the average 2–10 keV flux of the seven luminous obscured sources (from X-ray spectral fitting) in our sample ($\approx 1.8 \times 10^{-13} \text{ erg cm}^{-2} \text{ s}^{-1}$), we expect a surface density of $\approx 0.5 \text{ deg}^{-2}$ for Type 2 quasars from the La Franca et al. (2005) luminosity-dependent density evolution model (also see Cocchia et al., submitted). If we limit our study to the redshift range $\approx 0.3\text{--}0.8$ of the Zakamska et al. (2003) sample, then

the surface density of Type 2 quasars becomes $\approx 0.15 \text{ deg}^{-2}$ (R. Gilli, private communication; see also Gilli et al. 2006). Although our estimate of the surface density of SDSS Type 2 quasars is affected by significant uncertainties, it demonstrates that X-ray observations probably provide a more complete census of obscured quasar activity than that achieved at optical wavelengths. We note, in fact, that a sizable number of X-ray selected Type 2 quasars is not characterized by strong narrow emission lines (e.g., Mignoli et al. 2004).

4 SUMMARY OF THE RESULTS ON SDSS TYPE 2 QUASARS

In this paper we have reported new *Chandra* exploratory observations of six SDSS Type 2 quasar candidates at $z=0.49\text{--}0.73$ (which constitute the so-called “main” sample), selected among the most [O III] luminous objects from the Zakamska et al. (2003) sample, and provide results on two additional Type 2 quasar candidates serendipitously fallen in the same observations. We have also re-analysed archival *Chandra* and *XMM-Newton* observations of eight additional SDSS Type 2 quasar candidates which constitute, along with the above sources, the “extended” sample (for a total of 16 sources), thus providing a progress report on the X-ray properties of SDSS Type 2 quasars with respect to the preliminary results presented by V04. Although the strategy adopted to gain the final sample of 16 SDSS Type 2 quasars is quite varied, from Table 5 it appears evident that *Chandra* exploratory (<10 ks) on-axis observations are able to provide a significant fraction of X-ray detections (6/8, 75 per cent), but the fraction of sources with X-ray spectral information is clearly limited (3/6, 50 per cent). On the other side, the high-energy throughput allowed by the EPIC cameras on-board *XMM-Newton* guarantees, for obscured sources at relatively bright X-ray fluxes, good-quality X-ray spectra, at least at small off-axis angles (Table 5). The principal results can be summarized as follows:

- Ten of the “extended” sample of 16 SDSS Type 2 quasar candidates were detected either by *Chandra* or *XMM-Newton* (see Table 5). For seven of these sources, basic/moderate-quality X-ray spectral analysis has allowed us to achieve a direct measurement of the absorption ($\approx 10^{22}$ – a few 10^{23} cm^{-2}). These results are consistent with those obtained using *ROSAT* data and reported by V04.
- Using the [O III] line flux as an indicator of the intrinsic X-ray emission, as verified for the seven sources with higher X-ray statistics, we obtained indications that the X-ray undetected sources and the sources with a limited number of counts are possibly more obscured than those found absorbed through direct X-ray spectral fitting. This would imply that up to ≈ 50 per cent of the population is characterized by column densities $\gg 10^{23} \text{ cm}^{-2}$, with a sizable number of Compton-thick quasars possibly hiding among the X-ray faintest sources. This possibility is also suggested by the comparison of the X-ray-to-[O III] flux ratios of our sources vs. those obtained from a large sample of Seyfert 2 galaxies.

ACKNOWLEDGMENTS

CV and AC acknowledge partial support by the Italian Space agency under the contract ASI–INAF I/023/05/0. DMA is supported by the Royal Society. The authors would like to thank R. Gilli, M. Mignoli and G. Zamorani for useful discussions, M.

Guainazzi for providing data for Fig. 6, and the referee for his/her suggestions which helped us to improve the manuscript.

REFERENCES

- Abazajian K. et al., 2003, AJ, 126, 2081
Alexander D.M. et al., 2001, AJ, 122, 2156
Alexander D.M. et al., 2003, AJ, 126, 539
Antonucci R., 1993, ARA&A, 31, 473
Arnaud K.A., 1996, in Jacoby G., Barnes J., eds, ASP Conf. Ser. Vol. 101, Astronomical Data Analysis Software and Systems V. Astron. Soc. Pac., San Francisco, p. 17
Avni Y., 1976, ApJ, 210, 642
Barger A.J. et al., 2003, AJ, 126, 632
Bassani L., Dadina M., Maiolino R., Salvati M., Risaliti G., della Ceca R., Matt G., Zamorani G., 1999, ApJS, 121, 473
Bauer F.E., Alexander D.M., Brandt W.N., Schneider D.P., Treister E., Hornschemeier A.E., Garmire G.P., 2004, AJ, 128, 2048
Becker R.H., White R.L., Helfand D.J., 1995, ApJ, 450, 559
Brandt W.N., Hasinger G., 2005, ARA&A, 43, 827
Caccianiga A. et al., 2004, A&A, 416, 901
Cash W. 1979, ApJ, 228, 939
Cocchia F. et al., A&A, submitted
Collinge M.J., Brandt W.N., 2000, MNRAS, 317, L35
Comastri A. et al., 2001, MNRAS, 327, 781
Crawford C.S., Fabian A.C., Gandhi P., Wilman R.J., Johnstone R.M., 2001, MNRAS, 324, 427
Crawford C.S., Gandhi P., Fabian A.C., Wilman R.J., Johnstone R.M., Barger A.J., Cowie L.L., 2002, MNRAS, 333, 809
Dickey J.M., Lockman F.J., 1990, ARA&A, 28, 215
Fiore F. et al., 2003, A&A, 409, 79
Freeman P.E., Kashyap V., Rosner R., Lamb D.Q., 2002, ApJS, 138, 185
Gandhi P., Crawford C.S., Fabian A.C., Johnstone R.M., 2004, MNRAS, 348, 529
Garmire G.P., Bautz M.W., Ford P.G., Nousek J.A., Ricker G.R., 2003, Proc. SPIE, 4851, 28
Giacconi R. et al., 2002, ApJS, 139, 369
Gilli R., Salvati M., Hasinger G., 2001, A&A, 366, 407
Gilli R., Comastri A., Hasinger G., 2006, A&A, submitted
Guainazzi M., Fabian A.C., Iwasawa K., Matt G., Fiore F., 2005, MNRAS, 356, 295
Hickox R.C., Markevitch M., 2006, ApJ, 645, 95
La Franca F. et al., 2005, ApJ, 635, 864
Mainieri V. et al., 2002, A&A, 393, 425
Mainieri V. et al., 2005a, MNRAS, 356, 1571
Mainieri V. et al., 2005b, A&A, 437, 805
Maiolino R., Salvati M., Bassani L., Dadina M., della Ceca R., Matt G., Risaliti G., Zamorani G., 1998, A&A, 338, 781
Maiolino R. et al., 2006, A&A, 445, 457
Mignoli M. et al., 2004, A&A, 418, 827
Mulchaey J.S. et al., 1994, ApJ, 436, 586
Netzer H., Mainieri V., Rosati P., Trakhtenbrot B., 2006, A&A, 453, 525
Norman C. et al., 2002, ApJ, 571, 218
Nousek J.A., Shue D.R., 1989, ApJ, 342, 1207
Page K.L., Reeves J.N., O'Brien P.T., Turner M.J.L., 2005, MNRAS, 364, 195
Panessa F., Bassani L., Cappi M., Dadina M., Barcons X., Carrera F.J., Ho L.C., Iwasawa K., 2006, A&A, 455, 173
Perola G.C. et al., 2004, A&A, 421, 491
Piconcelli E., Jimenez-Bailón E., Guainazzi M., Schartel N., Rodríguez-Pascual P.M., Santos-Lleó M., 2005, A&A, 432, 15
Ptak A., Zakamska N.L., Strauss M.A., Krolik J.H., Heckman T.M., Schneider D.P., Brinkmann J., 2006, ApJ, 637, 147 (P06)
Reeves J.N., Turner M.J.L., 2000, MNRAS, 316, 234
Shemmer O., Brandt W.N., Vignali C., Schneider D.P., Fan X., Richards G.T., Strauss M.A., 2005, ApJ, 630, 729
Shemmer O. et al., 2006, ApJ, 644, 86
Spergel D.N. et al., 2003, ApJS, 148, 175
Stern D. et al., 2002, ApJ, 568, 71
Szokoly G.P. et al., 2004, ApJS, 155, 271
Vignali C., Alexander D.M., Comastri A., 2004a, MNRAS, 354, 720 (V04)
Vignali C., Alexander D.M., Comastri A., 2004b, proceedings of the 6th Italian National Meeting on AGN electronic edition at <http://www.arcetri.astro.it/~agn6/> (astro-ph/0409699)
Vignali C., Brandt W.N., Schneider D.P., Kaspi S., 2005, AJ, 129, 2519
Worsley M.A. et al., 2005, MNRAS, 357, 1281
York D.G. et al., 2000, ApJ, 120, 1579
Zakamska N.L. et al., 2003, ApJ, 126, 2125
Zakamska N.L., Strauss M.A., Heckman T.M., Ivezić Ž., Krolik J.H., 2004, AJ, 128, 1002
Zakamska N.L. et al., 2005, AJ, 129, 1212
Zakamska N.L. et al., 2006, AJ, in press (astro-ph/0603625)